Imaging the (un)imaginable of the Barrier Immune system

Guo, N.

Chapter 5

Immune Profiling of Psoriasis by Imaging Mass Cytometry

Nannan Guo[1], Mette Schreurs[1], Jeroen Eggermont[2], Elizabeth Kieras[3], David Eleuteri[3], Sharon Conder Niedecken[3], Christopher Ty[3], Boudewijn Lelieveldt[2], Noel F. C. C. de Miranda[4], Karen M. Page[3], Frits Koning[1] *

[1]Department of Immunology, Leiden University Medical Center, Leiden, The Netherlands
[2]Department of Radiology, Leiden University Medical Center, Leiden, The Netherlands
[3]Worldwide Research and Development, Pfizer Inc, Cambridge, Massachusetts, USA
[4]Department of Pathology, Leiden University Medical Center, Leiden, The Netherlands

*Correspondence

In preparation

Abstract

Psoriasis is a chronic inflammatory skin disorder characterized by keratinocyte hyperproliferation and differentiation combined with immune cell infiltration. Hereby, we applied imaging mass cytometry to profile the immune system in non-lesional and lesional skin biopsies from nine psoriasis patients. Snap-frozen skin sections were labelled with a 41-antibody panel followed by data acquisition on a Hyperion mass cytometer with 1 µm resolution. MCD™ Viewer was utilized to validate the staining quality of the IMC panel, and to visualize the tissue architecture. To characterize the immune compartment, we made use of HSNE-based pixel analysis in *Cytosplore Imaging* which allowed both the visualization of the structure of psoriatic skin, as well as the distribution and quantification of various T and myeloid cell subsets in the skin tissue samples. Moreover, we observed clusters of pixels harboring features of both T cells and myeloid cells (double feature pixels), presumably representing close contact between these two cell types. The results reveal a significant increase of the number of CD4 and CD8 T cells in lesional skin as well and an increase in the number of $CD206^+$ macrophages and $Fc\varepsilon RI^+$ mast cells. In contrast, no significant differences in the presence of dendritic cells (DCs) subsets were observed. However, double pixel analysis allowed the distinction of patients displaying frequent interactions between T cells and $CD207^+CD1c^+$ Langerhans-like DC in dermis. In addition, interactions between T cells and $CD207^-CD1c^+$ DC and between T cells and $CD206^+$ macrophages were observed in all patients but varied substantially. Thus, imaging mass cytometry in combination with pixel analysis allows classification of psoriasis patients based on differential presence of immune cell subtypes and interactions among those. Further work is needed to determine how this relates to disease severity and response to treatment.

Key terms: Imaging mass cytometry, IMC, CyTOF, Psoriasis

Introduction

Psoriasis (PS) is a common, chronic inflammatory skin disease with variations in severity depending on inheritance and environmental factors[1]. It is clinically characterized by the appearance of well-demarcated scaling erythematous plaques with thickened skin, and can affect joints and can be accompanied by a pro-inflammatory metabolic syndrome[2]. Psoriasis is an organ-specific autoimmune disease that is driven by the activated cellular immune system[3, 4], the pathophysiology of which is characterized by aberrant keratinocyte proliferation and immune cell infiltration in the dermis and epidermis in the lesional skin[5, 6, 7, 8]. Previous investigators have documented that macrophages and several populations of activated dendritic cells (DCs) were present in the inflamed skin[9, 10, 11, 12]. Immunofluorescence staining has shown that, compared to skin samples from healthy controls, psoriasis lesional skin has a higher level of tumor necrosis factor (TNF)-α producing $CD68^+$ macrophages - especially in early-phase psoriasis, while $CD68^+CD163^+$ macrophages are less abundant[13, 14]. In addition, IL-23 and IL-20 producing $CD11c^+$ DCs that express HLA-DR, CD40, and CD86, but lack the expression of the Langerhans cells (LCs) marker and the monocyte marker CD14 have the potential to activate T cells and keratinocytes to account for the progression of disease[15, 16, 17]. Moreover, patients with psoriasis showed increased presence of activated T-cells in skin lesions and PBMCs, the latter pointing to systemic activation[18, 19]. Flow cytometric analysis of blood showed the relationship between psoriasis disease severity (guttate, acute and chronic psoriasis) and different subsets of circulating CLA^+ T cells[20]. Single-cell RNA sequencing of rash-affected skin from psoriasis patients revealed active proliferative expansion of the regulatory T cells, tissue-resident memory T cells and exhausted $CD8^+$ T cells with a relative attenuation of antigen-presenting cells, suggesting involvement of these immune subsets in initiating and maintaining cutaneous inflammation[21, 22]. Moreover, the study in mice model system has clearly shown that locally activated and proliferating resident T cells are dependent on local TNF-α production, and are key players during the development of psoriatic lesions[23]. Infiltrating T cells in psoriasis lesions are mainly activated Type 1 T helper (Th1) and Th17 CD4 T cells[24, 25, 26].

The advances of high-dimensional imaging mass cytometry (IMC) approach offer new opportunities to simultaneously investigate diverse skin-resident immune cell populations of psoriasis with higher resolution than ever before in *situ*. Previously, we have developed an IMC-based approach which is able to detect more than 40 different heavy metal isotopes simultaneously, to profile and compare immune

systemic components and complexity in detail in the tissue context[27, 28, 29].

In this study, we applied IMC to skin biopsies from nine psoriasis patients to define the spatial orientation of the immune cells in the tissue context by a pixel-based analysis approach in *Cytosplore Imaging*. Firstly, we determined 16 separate clusters of skin immune population-associated pixels and calculated the percentage of each pixel-cluster in psoriasis. Here, we observed multiple clusters of pixels with features of both lymphoid and myeloid cells that were located in immune aggregates of lesional skin, pointing towards close cell-cell interactions related to the pro-inflammatory state in psoriatic lesions. Further analysis indicated the phenotype of the cells involved in these cell-cell interactions and revealed substantial patient heterogeneity, findings that might relate to psoriasis disease severity. Overall, our IMC data analysis at the pixel level provides a baseline for the identification of immune cell subsets, their distribution in *situ*, as well as their interactions, information that may be of relevance for the development of more targeted, patient-specific therapies.

Method

Tissue material

Both lesional and non-lesional skin samples from 9 psoriatic patients recruited by Pfizer Inc were included in this study. Patients were not receiving any conventional or biological systemic therapy at the time of sampling. The skin biopsies were embedded in optimal cutting temperature compound, snap-frozen in isopentane and stored at -80 °C. Baseline characteristics and disease course of these psoriatic patients were given in Table 1.

Mass cytometry antibodies preparation

Heavy metal isotope-labelled antibodies are listed in Table 2. Some antibodies were pre-conjugated (Fluidigm) while others were conjugated in-house with heavy metal isotopes using the Maxpar Antibody Labeling Kit and protocol (Fluidigm). The conjugation of antibodies against α-smooth muscle actin (αSMA) and collagen I with Cisplatin 194 and 198 were performed using a protocol adapted by Schulz et al[30]. CD31 was labelled with 209Bito using a protocol adapted by Spitzer et al[31].

Imaging Mass Cytometry staining

Imaging mass cytometry staining procedures on snap-frozen tissue were developed in our previous study[27]. Based on this the metal-tagged antibodies were used either for 2 hours at room temperature or overnight at 4°C as indicated in Table

2. IMC immunostaining was performed on all frozen skin samples from the nine patients in a single experiment. Tissue sections were dried at room temperature, followed by fixation with cold 1% paraformaldehyde (PFA) for 30 min at 4° C. Then, the skin sections were incubated with the first antibody mixture for 2 hours at room temperature (Table 2). After washing three times for 5 mins with staining buffer (0.5% BSA, 0.05% Tween in DPBS), the sections were incubated with the second antibody mixture overnight at 4°C (Table 2). Next, the sections were washed three times for 5 mins with staining buffer. Finally, the slides were washed one time for 2 mins with demineralized water, and dried under an air flow.

Imaging mass cytometry data acquisition

The entire skin sections were ablated at 200 Hz on a Helios time-of-flight mass cytometer coupled to a Hyperion Imaging System (Fluidigm). The Hyperion was autotuned using a 3-element tuning slide (Fluidigm) as described in the Hyperion imaging system user guide. The regions of interest (ROIs) per sample were selected based on hematoxylin and eosin (H&E) stains on consecutive slides. All raw data were analyzed for marker intensity based on the maximum signal threshold, defined at the 98th percentile of all pixels in a single ROI using Fluidigm MCD™ viewer (v1.0.560.2).

Imaging Mass Cytometry data analysis

Cytosplore Imaging facilitated the complete exploration pipeline in an integrated manner as described previously (Chapter 2). First, ome.TIFF files were exported from Fluidigm, and we applied the arcsin transformation with a cofactor of five upon loading the data sets to *Cytosplore imaging*. Next, we applied HSNE analysis[32] on all pixels from all ROIs which resulted in the clustering of pixels based on the marker expression profiles. Based on this tissue pixels were distinguished from background pixels followed by a second HSNE analysis of the tissue pixels to visualize the structural and cellular components in the skin tissue by projection of the resulting pixel clusters back onto the tissue section with the imaging viewer. Finally, we further refined the clustering by focusing on the $CD45^{+/dim}$ pixels and performed a t-SNE analysis for the immune markers. Using this approach, we could visualize T cells, $CD3^{-}CD7^{+}$ ILCs, B cells, DCs, macrophages and mast cells simultaneously in a single region. Strikingly, double features pixels were also identified and able to project onto skin tissue, to emphasize the interaction of myeloid cell subsets and lymphoid cells.

Results

Overview of the overall structure of lesional and non-lesional psoriatic skin by IMC

To survey the spatial distribution of the immune and non-immune compartments, IMC was performed on snap-frozen psoriatic skin sections using a 41-antibody panel. This panel contained structural (E-cadherin, Collagen I and α-smooth muscle actin (αSMA)), stromal (Vimentin and CD31), lymphocyte (CD3, CD20, CD7, CD4 and CD8a), and myeloid markers (CD11c, HLA-DR, CD207, CD1c, CD206, CD163) next to markers indicative of cellular differentiation, tissue residency, and cellular activation. Paired non-lesional and lesional skin samples from nine patients were included. Hematoxylin and eosin (H&E) staining of the skin samples (Figure 1A) yielded images that were highly similar to those obtained through of visualization DNA, Collagen I and αSMA staining by IMC; a representative patient sample is shown in Figure 1B. A further magnification of the image shows that the actual IMC image consists out of pixels (Figure 1B, lower images). We next employed *Cytosplore imaging* to analyze the expression patterns of all 41 markers simultaneously at the pixel level.

First we selected tissue-based pixels and performed an HSNE analysis based on the expression of E-cadherin, CD31, vimentin, Ki-67 and CD45 which yielded five major clusters of pixels representing the epidermis, vessels, stromal cells in the dermis, proliferating keratinocytes, and immune cells respectively (Figure 1C, D). Projection of these clusters back onto the tissue slide revealed the tissue architecture (Figure 1E), clearly demonstrating the thickening of the epidermis and an increase of Ki-67$^+$ keratinocytes in lesional skin compared to non-lesional skin. In addition, a significant increase and colocalization of CD31$^+$ endothelial and CD45$^+$ immune cells is evident in lesional skin (Figure 1E), while no apparent differences were observed between the presence of vimentin$^+$ stromal cells that were scattered throughout the dermis in both lesional and non-lesional skin (Figure 1E).

Thus, pixel-based analysis allows the visualization of the immune compartment within the tissue context.

Figure 1. The histologic analysis of psoriatic skin by H&E and IMC analysis. (A) H&E staining was performed on skin tissues of a psoriasis patient. **(B)** Overlay of DNA, Collagen I and αSMA to visualize the histology of skin by IMC analyzed in MCD™ Viewer. **(C-D)** Cellular pixels of skin were selected and clustered in *Cytosplore Imaging*. Colors represent the different cellular clusters in **(C)**. Colors represent relative expression of indicated markers in (**D**). **(E)** The main cellular components were projected back onto image in *Cytosplore imaging*. Colors represent indicated the various cellular components.

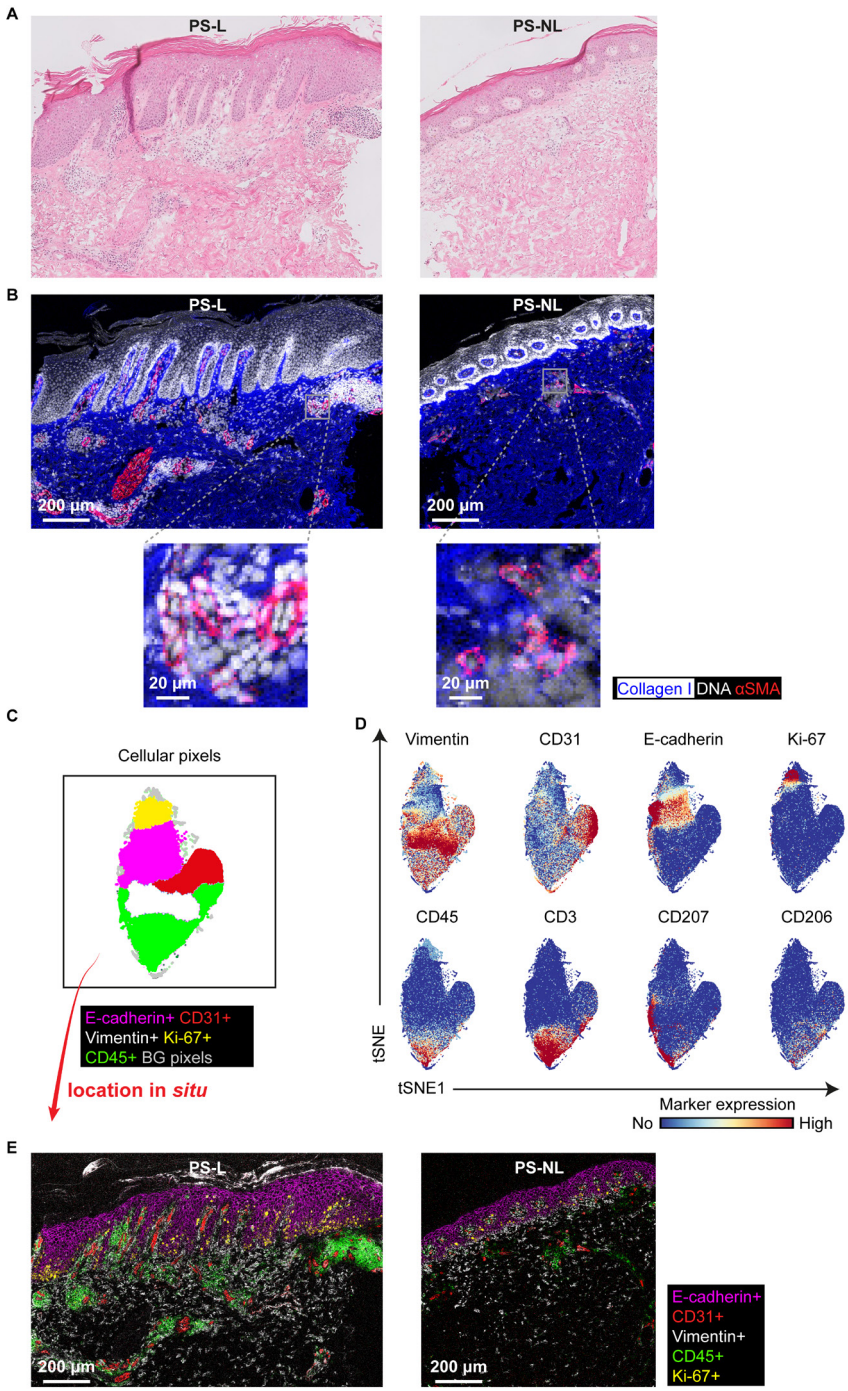

(Figure legend in previous page)

Immune cellular clusters of non-lesional and lesional psoriatic skin

To demonstrate the spatial organization of the immune cell subsets in *situ*, we performed an in-depth analysis of the $CD45^+$ immune cell-pixels, this identified 12 clusters of pixels in psoriatic skin, representing three T cell subsets ($CD3^+CD4^+$, $CD3^+CD8a^+$, $CD3^+CD4^-CD8a^-$), $CD3^-CD7^+$ innate lymphoid cells (ILCs), $CD20^+$HLA-DR^+ B cells, three DC subsets distinguished by differential expression of CD207 and CD1c, two subsets of macrophages ($CD206^+CD163^+$ and $CD206^+CD163^-$), and two mast cell sub-populations ($CD117^+$FceRIα^+ and $CD117^-$FceRIα^+) (Figure 2 and S1). Quantification of the number of pixels per immune cell subset demonstrates a significant increase of CD4 and CD8 T cells, macrophages and mast cells in lesional skin, while no significant differences were observed for the DC subsets (Figure 2B-E). The absence of CD45RA on the large majority of both CD4 and CD8 T cells indicates that these are predominantly memory T cells. Finally, $CD4^+$ T cells were more abundant as compared to $CD8^+$ T cells (Figure 2B). Visual inspection of the location of immune subset-specific pixels indicated that the majority of T cells, macrophages and mast cells were located in the dermis in both lesional and non-lesional skin samples (Figure 2F-I). Very few B cell and ILCs specific pixels were observed in both skin samples (Figure S1). As expected the majority of $CD207^+CD1c^-$ pixels, indicative of Langerhans cells, were located in the epidermis while the large majority dermal DC pixels were $CD207^-CD1c^+$ (Figure 2I).

Altogether, pixel analysis can be used to identify and visualize the spatial distribution of immune cell subsets. Moreover, it allows for unbiased pixel-based quantification of the presence of such subsets to facilitate the comparison of psoriatic non-lesional and lesional skin in *situ*.

Identification of pixel-clusters harboring features of both T and myeloid cells allow the quantification of immune interaction networks

As the generated images indicated substantial co-localization of T cells with myeloid cell types in the dermis of the lesional samples from psoriasis patients, we next aimed to further analyze and quantify such interactions in all patient samples.

Figure 2. Identification and quantification of immune subsets with pixel-based analysis of IMC images of lesional and non-lesional psoriatic skin samples. (A) A collective tSNE was performed on $CD45^{+/dim}$ pixels from the non-lesional and lesional skin of a representative psoriasis patient. Each dot represents a single pixel. Colors represent relative expression of the indicated immune markers. **(B-E)** Quantification of each immune subsets from nine psoriasis patients. **(F-I)** Display of spatial distribution of the identidied cell types in the non-lesional and lesional skin of a representative psoriasis patient. Error bars indicate mean ± s.e.m. *P < 0.05, ** P < 0.01, Wilcoxon signed-rank test for comparisons.

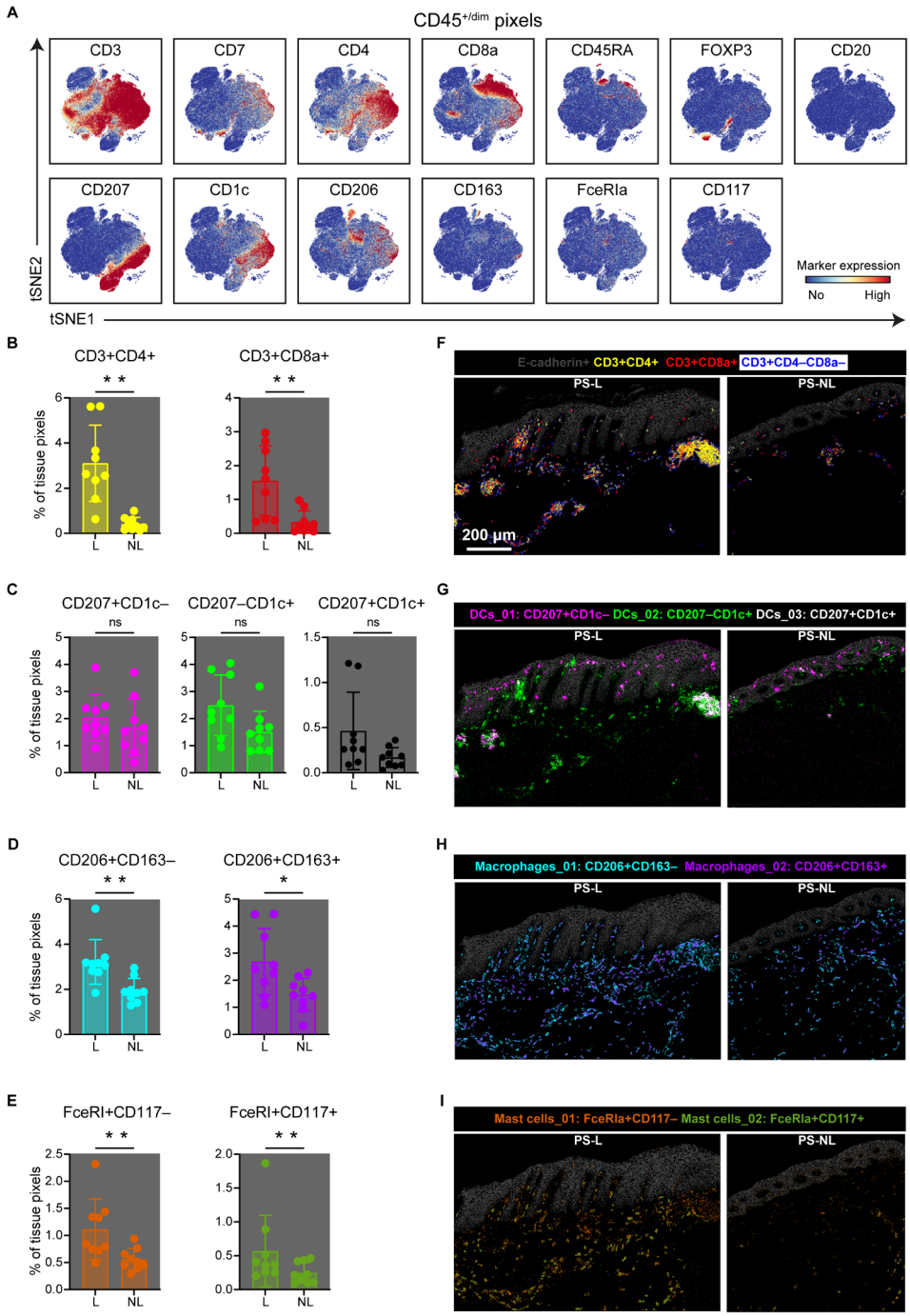

(Figure legend in previous page)

Here, we made use of clusters of pixels that harbored both T cell and myeloid markers, called double feature pixels hereafter. Figure 3 shows the distribution of $CD3^+$ pixels (red), $CD1c^+$ pixels (green), and $CD3^+CD1c^+$ double feature pixels (yellow) in a lesional skin section of a psoriatic patient, demonstrating the abundance of such double feature pixels in immune aggregates in the dermis. Further magnification of immune cell infiltrated area's indicates that these double feature pixels are predominantly found in between T cells and myeloid cells (Figure 3B) and thus likely represent close interactions between these two cell types.

Three types of double feature pixels could be readily identified in the HSNE-based pixel analysis pipeline, $CD3^+CD207^+CD1c^-$ (DCs_01&T), $CD3^+CD207^-CD1c^+$ (DCs_02&T), and $CD3^+CD207^+CD1c^+$ (DCs_03&T). We next quantified these double feature pixels in the lesional samples of the nine patients (Figure 4). For this we determined the total number of tissue pixels and the number of double feature pixels in each tissue sample and used this to calculate the percentage of double feature pixels (Figure 4A). Here, patients PS#08 and PS#09 had a high frequency of both DCs_02&T ($CD3^+CD207^-CD1c^+$) and DCs_03&T ($CD3^+CD207^+CD1c^+$) pixels, patients PS#4 and PS#6 had a high frequency of DCs_02&T pixels only, while the other patients exhibited a low frequency of both DCs_02&T and DCs_03&T (Figure 4A, B). Two pixel-clusters with features of T cells and macrophages were also identified in the lesional skin both of which were present in similar number sin patients samples (Figure 4C, S2). Interestingly, on patients PS#04, PS#08 and PS#09 a high proportion of pixels harboring features of T cells and macrophages were observed (Figure 4C).

Thus, pixel-based analysis of psoriasis skin samples allows the identification and quantification of cell-cell interactions that may underlie patients heterogeneity and disease severity.

Discussion

Psoriasis is an immune mediated inflammatory skin disease[33]. In our study, we analyzed non-lesional and lesional skin from patients with psoriasis to visualize the skin architecture and characterize the complexity of the innate and adaptive immune compartment in *situ* by IMC. Superior to conventional immunohistochemistry and immunofluorescence, IMC allows the detection of over 40 markers simultaneously. Therefore, the tissue context can be investigated with a higher resolution, for both the non-immune and immune compartments. Moreover, we used the in-house developed pixel-based approach, *Cytosplore*

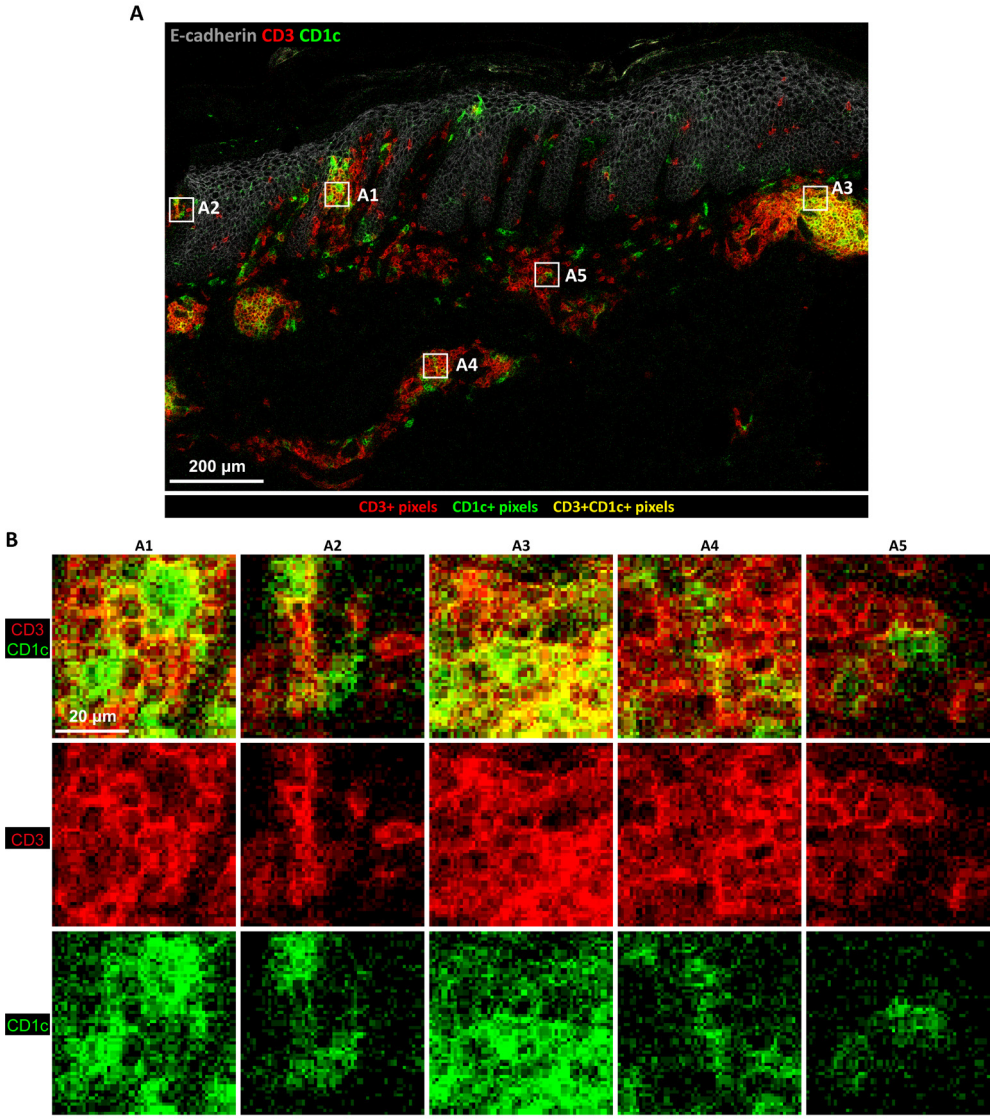

Figure 3. **Visualization of double feature pixels indicative of close proximity of T cells and DCs. (A)** Overlay by the staining of CD3 (red) and CD1c (green) in MCD™ Viewer visualize pixels that are CD3 and CD1c positive (yellow). **(B)** Magnification of the boxed areas in (A) with the individual markers as indicated.

Imaging, which was adapted from *Cytosplore*$^{+HSNE}$ [32], to visualize the composition and organization of immune cells for nine psoriasis patients. This allowed the identification of the various immune subsets in the skin samples. Moreover, the analysis of pixels harboring feature of both T cell and myeloid cells allowed the

identification, visualization and quantification of cell-cell interactions that may be related to disease severity.

Recently, the approaches based on cell segmentation analysis, like Imacyte[29] and Histocat[34] have been developed. Here, the creation of a single cell mask based on nuclei, cytoplasm/membrane, and background removal is necessary for each sample to allow for immunophenotyping within the spatial localization and subsequent neighborhood analysis[35]. However, due to differences in immune cell morphology and cell density variations in tissues, the true signal is frequently lost during the removal of background noise or cannot be exactly categorized into cells, particularly in areas where cells are densely packed. Here, pixel-based analysis provides an alternative that to identify cell subsets and quantify interactions between those.

Dendritic cells (DCs) are professional antigen presenting cells (APCs), and crucially involved in the initiation and propagation of adaptive immune responses to pathogens[36]. Langerhans cells (LCs) are unique as they are the only DC subset observed in the epidermis in normal skin[37]. During inflammation LCs become activated and transition through the dermis with differential expression of langerin, epithelial cell adhesion molecule (EpCam), CD11b and CD103[37]. Previous studies in mice models of skin infection identified three subset of skin DCs, LCs, Langerin $(CD207)^{+}$ dermal DCs, and classic dermal DCs. Here, LCs contribute to the generation of antigen-specific Th17 cells[38]. Recent studies have shown that IL-23 and IL-22 are important mediators in psoriasis skin inflammation[39, 40]. IL-23-producing macrophages and DCs are involved in the development of Th17 cells that have differentiated from naive T cells in the presence of IL-6 and TGF-β[41, 42]. Moreover, dermal macrophages are increased in psoriasis compared with normal skin[12], and have been shown to produce inflammatory TNF-α and inducible nitric oxide synthase (iNOS)[12, 43]. Moreover, many genes upregulated in activated macrophages have been found in psoriasis as well, including STAT1, CXCL9, Mx1, and HLA-DR[12]. Importantly, treatment with etanercept, a TNF receptor-immunoglobulin fusion protein, leads to a decrease in the presence of macrophages in psoriatic skin[44]. Altogether, the network of DCs and macrophages interacting with T cells in the skin lesion is a logical target for therapy of psoriasis.

According to the analysis of T and myeloid cells in psoriatic lesion, we identified three clusters of pixels of pixels harboring features of T cells and DCs based on the presence of CD3, langerin/CD207 and CD1c, suggesting crosstalk between T cells and various dermal DCs in the lesion. In addition, $CD206^{+}CD163^{+/-}$ macrophages

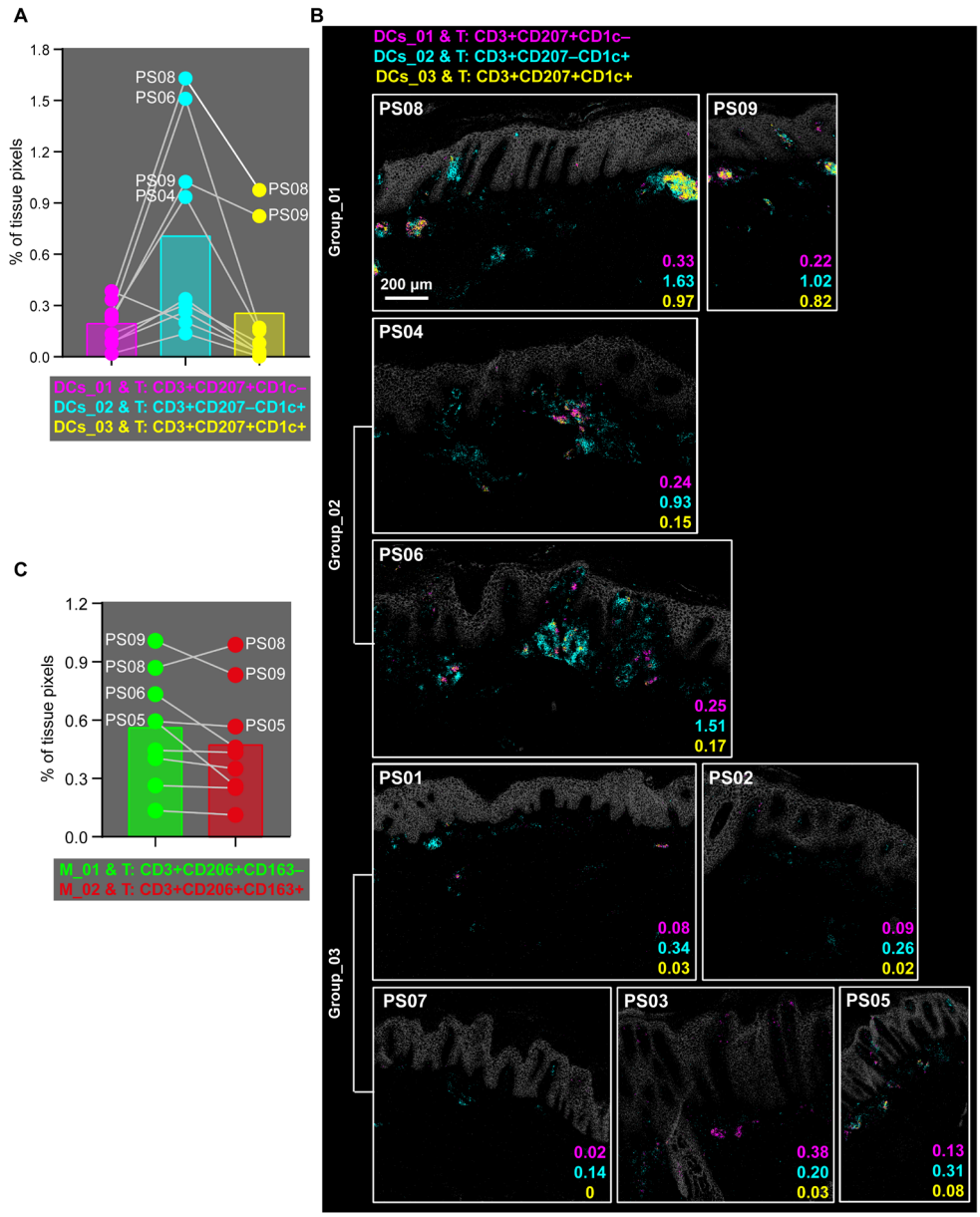

Figure 4. Identification and quantification of double feature pixelss in psoriatic lesions. (A-B) The quantification **(A)** and visualization **(B)** of three double feature pixel classes indicative of interaction between T and DCs in lesional skin samples. **(C)** The quantification of two double feature pixel classes indicative of interactions between T cells and macrophages in lesional skin samples. Colors represent different clusters as indicted.

were observed to colocalize with T cells in the lesion as well. Moreover, we observed substantial differences between the patients. A higher presence of pixels indicative of interaction between T cells and both DCs and macrophages were observed in patients PS#08 and PS#09, while much less evidence for such interactions was observed in other patients. However, at present we did not find a correlation between the clinical scores and our observations (Table 1). Possibly, this could be due to the fact that the Psoriasis Area and Severity Index (PASI) score is related to the overall assessment of the patient and may not reflect the actual severity in the skin lesion region investigated. However, our results indicate that substantial differences can be detected between patients. Further studies with larger sample sizes will be needed to explore the possible correlation with disease severity. Future work will be also required to elucidate the functional profile of the cell subsets with more advanced IMC antibody panels, mRNA analysis and functional studies.

Collectively, the current study provides an alternative, pixel-based analysis method for IMC datasets, especially suitable for tissue samples with densely packed cells. Moreover, we showed the composition and distribution of immune subsets *in situ* for psoriasis patients, and different patterns of colocalization of T cells and myeloid cells. Our work provided a reference basis to better understand immune profiling of psoriasis, and may potentially facilitate improved prognosis and treatment of psoriasis.

Funding

This research was supported by BIOMAP (Bio-markers in Atopic Dermatitis and Psoriasis), a project funded by the Innovative Medicines Initiative 2 Joint Undertaking under grant agreement no. 821511 (NG and FK). N.F.C.C.d.M. is funded by the European Research Council (ERC) under the European Union's Horizon 2020 Research and Innovation Programme (grant agreement no. 852832).

Acknowledgements

We thank the patients. We thank all operators in the Flow Cytometry Core Facility of the LUMC for technical assistance with measurements on Helios and Hyperion.

Authorship Contributions

NG and FK conceived the study and wrote the manuscript. NG performed most experiments with the help of MS and NFCCdM. NG performed most of the analyses with the help of FK, JE and BL. EK, DE, SCN, CT and KMP collected skin biopsies from psoriasis patients. All authors discussed the results and commented on the manuscript.

Reference

1. Green, M.S., Prystowsky, J.H., Cohen, S.R., Cohen, J.I. & Lebwohl, M.G. Infectious complications of erythrodermic psoriasis. *J Am Acad Dermatol* **34**, 911-914 (1996).
2. Griffiths, C.E. & Barker, J.N. Pathogenesis and clinical features of psoriasis. *Lancet* **370**, 263-271 (2007).
3. Lebwohl, M. Psoriasis. *Lancet* **361**, 1197-1204 (2003).
4. Lowes, M.A., Bowcock, A.M. & Krueger, J.G. Pathogenesis and therapy of psoriasis. *Nature* **445**, 866-873 (2007).
5. Bowcock, A.M. & Krueger, J.G. Getting under the skin: the immunogenetics of psoriasis. *Nat Rev Immunol* **5**, 699-711 (2005).
6. Boyman, O. *et al.* Activation of dendritic antigen-presenting cells expressing common heat shock protein receptor CD91 during induction of psoriasis. *Br J Dermatol* **152**, 1211-1218 (2005).
7. Lew, W., Bowcock, A.M. & Krueger, J.G. Psoriasis vulgaris: cutaneous lymphoid tissue supports T-cell activation and "Type 1" inflammatory gene expression. *Trends Immunol* **25**, 295-305 (2004).
8. Krueger, J.G. The immunologic basis for the treatment of psoriasis with new biologic agents. *J Am Acad Dermatol* **46**, 1-23; quiz 23-26 (2002).
9. Nestle , F.O. *et al.* Plasmacytoid predendritic cells initiate psoriasis through interferon-α production. *Journal of Experimental Medicine* **202**, 135-143 (2005).
10. Lowes, M.A. *et al.* Increase in TNF-α and inducible nitric oxide synthase-expressing dendritic cells in psoriasis and reduction with efalizumab (anti-CD11a). *Proceedings of the National Academy of Sciences* **102**, 19057-19062 (2005).
11. Krueger, J.G. The immunologic basis for the treatment of psoriasis with new biologic agents. *Journal of the American Academy of Dermatology* **46**, 1-26 (2002).
12. Fuentes-Duculan, J. *et al.* A subpopulation of CD163-positive macrophages is classically activated in psoriasis. *J Invest Dermatol* **130**, 2412-2422 (2010).
13. Leite Dantas, R. *et al.* Macrophage-mediated psoriasis can be suppressed by regulatory T lymphocytes. *J Pathol* **240**, 366-377 (2016).
14. Kamata, M. & Tada, Y. Dendritic Cells and Macrophages in the Pathogenesis of Psoriasis. *Front Immunol* **13**, 941071 (2022).
15. Lee , E. *et al.* Increased Expression of Interleukin 23 p19 and p40 in Lesional Skin of Patients with Psoriasis Vulgaris. *Journal of Experimental Medicine* **199**, 125-130 (2004).
16. Wang, F. *et al.* Prominent Production of IL-20 by CD68+/CD11c+ Myeloid-Derived Cells in Psoriasis: Gene Regulation and Cellular Effects. *Journal of Investigative Dermatology* **126**, 1590-1599 (2006).
17. Lowes, M.A. *et al.* Increase in TNF-alpha and inducible nitric oxide synthase-expressing dendritic cells in psoriasis and reduction with efalizumab (anti-CD11a). *Proc Natl Acad Sci U S A* **102**, 19057-19062 (2005).
18. Czarnowicki, T. *et al.* Skin-homing and systemic T-cell subsets show higher activation in atopic dermatitis versus psoriasis. *J Allergy Clin Immunol* **136**, 208-211 (2015).
19. Guttman-Yassky, E. & Krueger, J.G. Atopic dermatitis and psoriasis: two different immune diseases or one spectrum? *Current Opinion in Immunology* **48**, 68-73 (2017).
20. Ferran, M., Giménez-Arnau, A.M., Bellosillo, B., Pujol, R.M. & Santamaria-Babi, L.F. Circulating CLA+ T cell subsets inversely correlate with disease severity and extension in acute psoriasis but not in chronic plaque psoriasis. *Eur J Dermatol* **18**, 647-650 (2008).
21. Liu, J. *et al.* Single-cell RNA sequencing of psoriatic skin identifies pathogenic Tc17 cell subsets and reveals distinctions between CD8(+) T cells in autoimmunity and cancer. *J Allergy Clin Immunol* **147**, 2370-2380 (2021).
22. Liu, Y. *et al.* Classification of human chronic inflammatory skin disease based on single-cell immune profiling. *Sci Immunol* **7**, eabl9165 (2022).
23. Boyman, O. *et al.* Spontaneous development of psoriasis in a new animal model shows an essential role for resident T cells and tumor necrosis factor-alpha. *J Exp Med* **199**, 731-736 (2004).
24. Austin, L.M., Ozawa, M., Kikuchi, T., Walters, I.B. & Krueger, J.G. The Majority of Epidermal T Cells in Psoriasis Vulgaris Lesions can Produce Type 1 Cytokines, Interferon-γ, Interleukin-2, and Tumor Necrosis Factor-α, Defining TC1 (Cytotoxic T Lymphocyte) and TH1 Effector Populations:1 a Type 1 Differentiation Bias is also Measured in Circulating Blood T Cells in Psoriatic Patients. *Journal of Investigative Dermatology* **113**, 752-759 (1999).
25. Kim, J. & Krueger, J.G. Highly Effective New Treatments for Psoriasis Target the IL-23/Type 17 T Cell Autoimmune Axis. *Annual Review of Medicine* **68**, 255-269 (2017).
26. Noda, S. *et al.* The Asian atopic dermatitis phenotype combines features of atopic dermatitis and psoriasis with increased TH17 polarization. *Journal of Allergy and Clinical Immunology* **136**, 1254-1264 (2015).
27. Guo, N. *et al.* A 34-Marker Panel for Imaging Mass Cytometric Analysis of Human Snap-Frozen Tissue. *Frontiers in Immunology* **11** (2020).
28. Ijsselsteijn, M.E., Somarakis, A., Lelieveldt, B.P.F., Höllt, T. & de Miranda, N.F.C.C. Semi-automated background removal limits data loss and normalizes imaging mass cytometry data. *Cytometry*

Part A **99**, 1187-1197 (2021).
29. Somarakis, A., Van Unen, V., Koning, F., Lelieveldt, B. & Hollt, T. ImaCytE: Visual Exploration of Cellular Micro-Environments for Imaging Mass Cytometry Data. *IEEE Trans Vis Comput Graph* **27**, 98-110 (2021).
30. Schulz, A.R. & Mei, H.E. Surface Barcoding of Live PBMC for Multiplexed Mass Cytometry. *Methods Mol Biol* **1989**, 93-108 (2019).
31. Spitzer, M.H. *et al.* Systemic Immunity Is Required for Effective Cancer Immunotherapy. *Cell* **168**, 487-502.e415 (2017).
32. van Unen, V. *et al.* Visual analysis of mass cytometry data by hierarchical stochastic neighbour embedding reveals rare cell types. *Nature Communications* **8**, 1740 (2017).
33. Liang, Y., Sarkar, M.K., Tsoi, L.C. & Gudjonsson, J.E. Psoriasis: a mixed autoimmune and autoinflammatory disease. *Curr Opin Immunol* **49**, 1-8 (2017).
34. Schapiro, D. *et al.* histoCAT: analysis of cell phenotypes and interactions in multiplex image cytometry data. *Nat Methods* **14**, 873-876 (2017).
35. Ijsselsteijn, M.E., Somarakis, A., Lelieveldt, B.P.F., Höllt, T. & de Miranda, N. Semi-automated background removal limits data loss and normalizes imaging mass cytometry data. *Cytometry A* **99**, 1187-1197 (2021).
36. Banchereau, J. *et al.* Immunobiology of Dendritic Cells. *Annual Review of Immunology* **18**, 767-811 (2000).
37. Kaplan, D.H. In vivo function of Langerhans cells and dermal dendritic cells. *Trends in Immunology* **31**, 446-451 (2010).
38. Igyártó, B.Z. *et al.* Skin-resident murine dendritic cell subsets promote distinct and opposing antigen-specific T helper cell responses. *Immunity* **35**, 260-272 (2011).
39. Ma, H.L. *et al.* IL-22 is required for Th17 cell-mediated pathology in a mouse model of psoriasis-like skin inflammation. *J Clin Invest* **118**, 597-607 (2008).
40. Lowes, M.A. *et al.* Psoriasis vulgaris lesions contain discrete populations of Th1 and Th17 T cells. *J Invest Dermatol* **128**, 1207-1211 (2008).
41. Zheng, Y. *et al.* Interleukin-22, a T(H)17 cytokine, mediates IL-23-induced dermal inflammation and acanthosis. *Nature* **445**, 648-651 (2007).
42. McKenzie, B.S., Kastelein, R.A. & Cua, D.J. Understanding the IL-23-IL-17 immune pathway. *Trends Immunol* **27**, 17-23 (2006).
43. Verma, D. *et al.* Enhanced Inflammasome Activity in Patients with Psoriasis Promotes Systemic Inflammation. *J Invest Dermatol* **141**, 586-595.e585 (2021).
44. Zaba, L.C. *et al.* Amelioration of epidermal hyperplasia by TNF inhibition is associated with reduced Th17 responses. *J Exp Med* **204**, 3183-3194 (2007).

Supplementary information

Tables

Table 1 The clinical characteristics for psoriasis patients/skin lesional samples.

Patient No.	Sex	Age	BSA[1]	PASI[2]
PS#01	Male	45	6	8.2
PS#02	Female	23	4	7.2
PS#03	Male	34	4	6.3
PS#04	Male	61	7	8.2
PS#05	Male	55	4	5.8
PS#06	Male	69	3	4.2
PS#07	Female	56	5	3.6
PS#08	Male	54	6	9
PS#09	Female	56	5	6.4

[1]Score of Body Surface Area (BSA) with Psoriasis

[2]Higher PASI scores representing increasing severity of psoriasis

Table 2 Imaging mass cytometry antibody panel on the skin samples from psoriasis patients.

	Antigen	Tag	Clone	Supplier	Dilution	Incubation
1	CD94	141 Pr	DX22	Biolegend	50	RT
2	CD94	141 Pr	HP-3D9	BD Biosciences	50	RT
3	CXCR1	152Sm	5A12	BD Biosciences	50	RT
4	CD127	158 Gd	R34.34	Beckman	50	RT
5	PD-L1	150Nd	SP142	Fluidigm	50	RT
6	CD66b	163Dy	6/40c	Biolegend	50	RT
7	PD-1	165Ho	EH12.2H7	Fluidigm	50	RT
8	CD45RO	173Yb	UCHL1	Biolegend	50	RT
9	CD56	176Yb	NCAM16.2	Fluidigm	50	RT
10	CD207	148 Nd	4C7	Biolegend	100	RT
11	CD206	172Yb	19.2	BD Biosciences	100	RT
12	CD45	89Y	HI30	Fluidigm	50	4 °C
13	CD103	155Gd	Ber-ACT8	Biolegend	50	4 °C
14	CD1a	115In	010	Dako	50	4 °C
15	FcεRIα	143Nd	AER-37 (CRA-1)	Biolegend	50	4 °C
16	CD69	144Nd	FN50	Fluidigm	50	4 °C
17	CD4	145Nd	RPA-T4	Fluidigm	50	4 °C
18	CD8a	146Nd	RPA-T8	Fluidigm	50	4 °C
19	CD117	147Sm	104D2	Biolegend	50	4 °C
20	CD27	149Sm	O323	Biolegend	50	4 °C
21	CD123	151Eu	6H6	Fluidigm	50	4 °C
22	CD86	156Gd	IT2.2	Fluidigm	50	4 °C
23	E-cadherin	159Tb	67A4	Biolegend	50	4 °C
24	CD172a	160 Gd	15-414	Biolegend	50	4 °C
25	CD20	161Dy	H1	Fluidigm	50	4 °C
26	CD11c	162Dy	S-HCL-3	Biolegend	50	4 °C
27	CD11c	162Dy	Bu15	Fluidigm	50	4 °C
28	CD161	164Dy	HP-3G10	Fluidigm	50	4 °C
29	Granzyme B	167Er	GB11	Fluidigm	50	4 °C
30	CD1c	171Yb	L161	Biolegend	50	4 °C
31	CD25	175Lu	24204	Thermo Fisher	50	4 °C
32	FOXP3	142Nd	236A/E7	Thermo Fisher	100	4 °C
33	CD7	153Eu	CD7-6B7	Fluidigm	100	4 °C
34	CD163	154Sm	GHI/61	Fluidigm	100	4 °C
35	CD45RA	169Tm	HI100	Fluidigm	100	4 °C
36	CD3	170Er	UCHT1	Fluidigm	100	4 °C
37	CD57	174Yb	HNK-1	Biolegend	100	4 °C
38	αSMA	194Pt	1A4	CST	100	4 °C
39	Collagen I	196Pt	Polyclonal	Millipore	100	4 °C
40	Vimentin	198Pt	WM59	Biolegend	100	4 °C
41	CD31	209Bi	WM59	Biolegend	100	4 °C
42	Ki-67	166Er	D3B5	CST	200	4 °C
43	HLA-DR	168Er	L243	Biolegend	800	4 °C
Cell Signaling Technology (CST)						

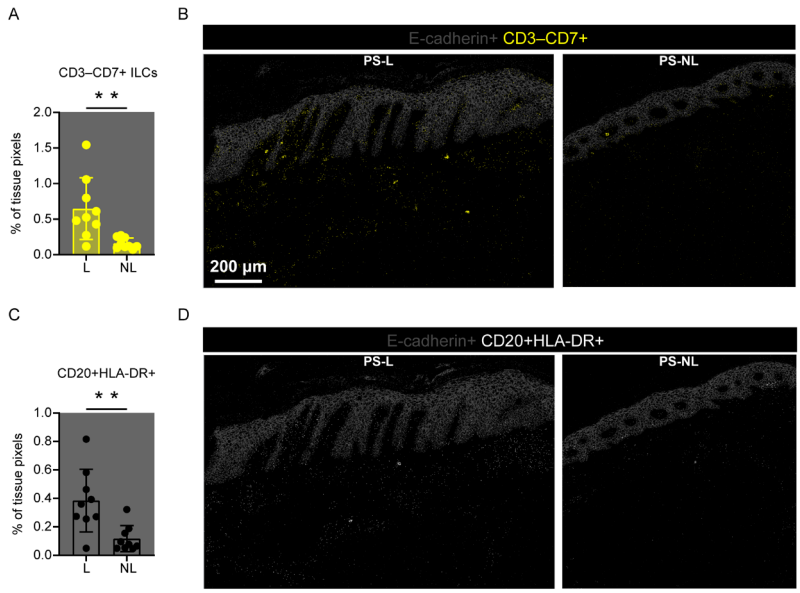

Figure S1. Quantification of pixels of CD3^{-}CD7^{+} ILCs and B cells from nine psoriasis patients and display of spatial distribution on the non-lesional and lesional skin of a representative psoriasis patient. Error bars indicate mean ± s.e.m. ** P < 0.01, Wilcoxon signed-rank test for comparisons.

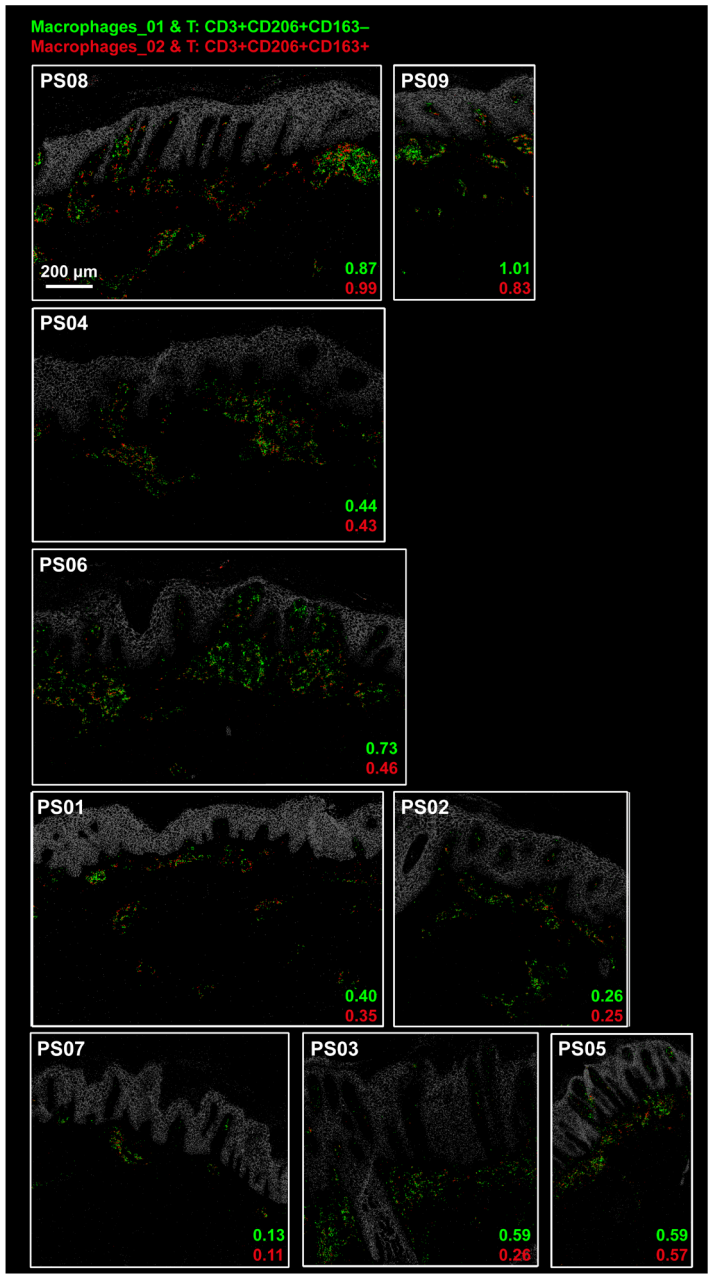

Figure S2. Visualization of two pixel-clusters harboring features of T cells and macrophages in lesional skin samples from psoriasis patients.